

Quasi-SU(3) truncation scheme for odd-even sd -shell nuclei.

C. E. Vargas^{1*}, J. G. Hirsch^{2†}, J. P. Draayer^{3‡}

¹ Departamento de Física, Centro de Investigación y de Estudios Avanzados del IPN,
Apartado Postal 14-740 México 07000 DF, México

² Instituto de Ciencias Nucleares, Universidad Nacional Autónoma de México,
Apartado Postal 70-543 México 04510 DF, México

³ Department of Physics and Astronomy, Louisiana State University,
Baton Rouge, LA 70803-4001, USA

November 21, 2018

Abstract

Abstract The quasi-SU(3) symmetry, as found in shell model calculations [1], refers to the dominance of the single particle plus quadrupole - quadrupole terms in the Hamiltonian used to describe well deformed nuclei, and to the subspace relevant in its diagonalization. It provides a very efficient basis truncation scheme. It is shown that a small number of SU(3) coupled irreps, those with the largest C_2 values within the direct product of the proton and neutron SU(3) irreps with spin 0 and 1 (for even number of particles), and spin 1/2 and 3/2 for (for odd number of nucleons), are enough to describe the low energy spectra and B(E2) transition strengths of ^{21}Ne , ^{23}Na and ^{25}Mg . A simple but realistic Hamiltonian is employed. Results compare favorably both with experimental data and with full shell model

*Electronic address: cvargas@fis.cinvestav.mx; fellow of CONACyT.

†Electronic address: hirsch@nuclecu.unam.mx

‡Electronic address: draayer@lsu.edu

calculations. Limitations and possible improvements of the schematic Hamiltonian are discussed.

PACS numbers: 21.60.Fw, 21.60.Cs, 27.70.+q

Keywords: Quasi-SU(3) symmetry, energies, B(E2) values, ^{21}Ne , ^{23}Na and ^{25}Mg .

1 Introduction.

Since its introduction more than fifty years ago [2], the shell model has been a fundamental tool in the microscopic description of nuclear properties. Full shell model calculations in the *sd*- [3] and *fp*-shells [1] provide very accurate predictions for energy levels, electromagnetic transition strengths and weak decay half lives. State of the art codes allow studies up to $A = 50$ [4]. The system symmetries, although in general are not exact, provide a natural truncation scheme of the Hilbert space while keeping the predictive power of the theory, and provide a qualitative understanding of collective nuclear modes. Algebraic models are particularly well suited to describe systems with symmetries, using either bosonic representations [5], fermionic representations [6, 7], or combination of both [8].

In the present article we concentrate our attention in the fermionic SU(3) algebraic model developed by Elliott [6]. Based on the crucial role the quadrupole - quadrupole interaction plays in deformed systems, the SU(3) algebra is the natural language to describe quadrupole excitations in a harmonic oscillator basis in light nuclei. The pseudo SU(3) model [7], built over the pseudo spin symmetry, plays a similar role in heavy deformed nuclei. Used as an approximate symmetry, i.e. allowing the mixing of different irreducible representations (irreps) through the single particle energies and the pairing interaction, it provides a very good description of low energy bands, B(E2) and B(M1) transition strengths in the rare earth region, both for even-even [9] and A-odd [10] deformed nuclei.

In the pseudo SU(3) model the truncation of the Hilbert space usually excludes intruder orbits, which are known to provide an important contribution to the total quadrupole moment. The quasi SU(3) truncation scheme [1] offers a simple and consistent way to include intruder orbits in the SU(3) description of heavy deformed nuclei. In [11] it was shown that including

the leading SU(3) irreps (those with the largest C_2 values) and spin 0 and 1 the interplay between the quadrupole - quadrupole interaction and the spin - orbit splitting is well described. A detailed description of four even-even nuclei in the sd -shell, ranging from ^{20}Ne to ^{28}Si was presented in [12]. Three odd-odd nuclei in the sd -shell are discussed in [13]. The present article deals with the odd-mass nuclei in the sd -shell. In the three cases the main goal is to prove that in well deformed nuclei, even in the presence of a large spin-orbit splitting, it is possible to make a good description of the low energy spectra using a small number of SU(3) irreps. This is the meaning of the “quasi SU(3) truncation scheme”. The results presented here and in the two accompanying articles strongly support this conclusion. They open the possibility for a coherent description of nucleons in normal and intruder levels in heavy deformed nuclei using the SU(3) formalism, as envisioned in [1].

In the present paper the low energy spectra and B(E2) transition strengths of ^{21}Ne , ^{23}Na and ^{25}Mg are studied using the quasi SU(3) basis and a schematic Hamiltonian. The band structure is recovered and the wave functions along each band are presented. Results are compared both with the experimental data and with full shell model calculations [3]. Section 2 reviews the essentials of the SU(3) model, including a short description of the SU(3) basis and the Hamiltonian. In sections 3, 4, and 5 the energy spectra, band structure and B(E2) transition strengths of ^{21}Ne , ^{23}Na and ^{25}Mg , respectively, are presented. Section 6 contains the conclusions.

2 The SU(3) model

For a general review of the SU(3) model and the operator expansion in terms of SU(3) tensors we refer the reader to references [6, 14, 15, 16, 17], as well as to the first article in this series [12]. In what follows we introduce the SU(3) basis and the schematic Hamiltonian used in this work.

The basis states are written as

$$|\{n_\pi[f_\pi]\alpha_\pi(\lambda_\pi, \mu_\pi), n_\nu[f_\nu]\alpha_\nu(\lambda_\nu, \mu_\nu)\}\rho(\lambda, \mu)kL\{S_\pi, S_\nu\}S; JM\rangle \quad (1)$$

where n_π is the number of valence protons in the sd -shell and $[f_\pi]$ is the irrep of the U(2) spin group for protons, which is associated with the spin $S_\pi = (f_\pi^1 - f_\pi^2)/2$. The SU(3) irrep for protons is (λ_π, μ_π) with a multiplicity label α_π associated with the reduction from $U(6)$. Similar definitions hold

$(\lambda_\pi, \mu_\pi)S_\pi$	C_2	$(\lambda_\nu, \mu_\nu)S_\nu$	C_2
(4,0)0	28	(4,1)1/2	36
(2,1)1	16	(2,2)1/2	24
(0,2)0	10	(3,0)3/2	18
		(0,3)3/2	18
		(1,1)1/2	9

Table 1: Irreps, spins and C_2 values for protons and neutrons in ^{21}Ne .

for the neutrons, labeled with ν . There are other two multiplicity labels: ρ , which counts how many times the total irrep (λ, μ) occurs in the direct product $(\lambda_\pi, \mu_\pi) \otimes (\lambda_\nu, \mu_\nu)$ and K , which classifies the different occurrences of the orbital angular momentum L in (λ, μ) .

The vector states (1) span the complete shell-model space within only one active (harmonic oscillator) shell for each kind of nucleon. As an example we take ^{21}Ne . It has two protons ($n_\pi = 2$) in the sd -shell, which can be accommodated in three possible irreps: $(\lambda_\pi, \mu_\pi) = (4,0)$, $(2,1)$ and $(0,2)$. The first and third irreps have spin zero, the second one has spin 1. Each one occurs only once ($\alpha_\pi = 1$). For three neutrons in the sd -shell there are five irreps: $(\lambda_\nu, \mu_\nu) = (4,1)$, $(2,2)$, $(3,0)$, $(0,3)$ and $(1,1)$. Three of them have spin 1/2, the other two have spin 3/2. The $\text{SU}(3)$ irreps are ordered by decreasing values of the expectation value of the second order Casimir operator, C_2 ,

$$\langle (\lambda, \mu) | C_2 | (\lambda, \mu) \rangle = (\lambda + \mu + 3) (\lambda + \mu) - \lambda\mu. \quad (2)$$

Proton and neutron irreps in ^{21}Ne are listed in Table 1 with their spin and C_2 values.

Calculations performed using the full proton-neutron coupled $\text{SU}(3)$ Hilbert space in the sd -shell [11, 12] show that the quasi $\text{SU}(3)$ [1] truncation scheme is quite efficient. The $\text{SU}(3)$ basis is built by taking the direct product of the proton and neutron irreps with the largest C_2 values and $S = 0$ and 1 (for even number of nucleons) or 1/2 and 3/2 (for odd number), and keeping from this list only those states with the largest total C_2 values [11, 12, 18]. The proton and neutron representations of each studied nuclei are shown in Tables 1, 5, and 8, and the truncated list of their final couplings, which describes the Hilbert space used for each nuclei, can be seen in Tables 3, 6, and 9.

Nucleus	χ	$G_\pi = G_\nu$	a	b	A_{sym}
^{21}Ne	0.1063	0.4524	-0.200	-0.020	0.010
^{23}Na	0.0914	0.4130	0	-0.005	0
^{25}Mg	0.0795	0.3800	-0.130	0.090	0.024

Table 2: Hamiltonian parameters in MeV.

The Hamiltonian used is

$$\begin{aligned}
H = & H_{sp,\pi} + H_{sp,\nu} - \frac{1}{2} \chi Q \cdot Q - G_\pi H_{pair,\pi} \\
& - G_\nu H_{pair,\nu} + a K_J^2 + b J^2 + A_{sym} C_2.
\end{aligned} \tag{3}$$

where $H_{sp,\alpha}$ is the spherical Nilsson Hamiltonian for $\alpha = \pi$ or ν and the quadrupole-quadrupole and pairing interaction strengths χ , G_π and G_ν has been fixed from systematics as in previous work [10, 12]. The parameters a , b , and A_{sym} correspond to the three ‘‘rotor terms’’. They are small, and provide some freedom to perform a nuclei by nuclei best fit. The Hamiltonian parameters used in this work are listed in Table 2.

For the spherical Nilsson Hamiltonian

$$H_{sp,\alpha} = \hbar\omega_o \left\{ \left(\hat{n} + \frac{3}{2} \right) - 2\kappa \vec{l} \cdot \vec{s} - \kappa\mu \vec{l}^2 \right\} \tag{4}$$

the Ring and Schuck [19] parametrization $\kappa = 0.08$ and $\mu = 0.000$ was chosen. While both the single particle Hamiltonian and the pairing terms induce a mixing of SU(3) irreps, for the values used here the single particle terms are by far and away the driving force behind the mixing.

Hamiltonian (3) proved to be very powerful in the description of the normal parity bands in heavy deformed A-odd nuclei [10], where protons and neutrons occupy different major shells. In the description of light nuclei, the same Hamiltonian is missing the proton-neutron pairing term, and for this reason it is not isoscalar. Given that the main goal of the present work is to assert the validity of the quasi SU(3) truncation scheme, we have kept this Hamiltonian, using its rotor terms to partially compensate for the missing terms. Further applications of this model to light and medium mass nuclei must use an isospin invariant Hamiltonian if the model is intended to display its full predictive power.

$(\lambda_\pi, \mu_\pi)S_\pi$	$(\lambda_\nu, \mu_\nu)S_\nu$	$(\lambda, \mu)S$ total			
(4,0)0	(4,1)1/2	(8,1)1/2	(6,2)1/2	(7,0)1/2	(4,3)1/2
(4,0)0	(2,2)1/2	(6,2)1/2	(4,3)1/2		
(2,1)1	(4,1)1/2	(6,2)1/2,3/2	(7,0)1/2,3/2	(4,3)1/2,3/2	
(4,0)0	(3,0)3/2	(7,0)3/2			
(4,0)0	(0,3)3/2	(4,3)3/2			
(2,1)1	(2,2)1/2	(4,3)1/2,3/2			
(0,2)0	(4,1)1/2	(4,3)1/2			

Table 3: The 17 irreps used in description of ^{21}Ne . In some couplings the total irrep can have spins of 1/2 and/or 3/2.

In the following sections a detailed analysis of the nuclei ^{21}Ne , ^{23}Na and ^{25}Mg is presented. The energy spectra, band structure and B(E2) transition strengths are shown in each case.

3 ^{21}Ne

^{21}Ne has two protons and three neutrons occupying the sd valence shell. As discussed in the previous section, they can be in any of the three SU(3) proton irreps and five SU(3) neutron irreps listed in Table 1, which include proton states with spin 0 and 1, and neutron states with spin 1/2 and 3/2. The truncated proton-neutron coupled basis is listed in Table 3. It includes the 17 coupled irreps with the largest C_2 values.

The ^{21}Ne energy spectra obtained with this basis using the Hamiltonian parameters shown in the first row of Table 2 are presented in the right hand side column of Fig. 1. They are compared with the experimental results [20], shown in the second column, and with the theoretical results obtained with full shell model calculations using the unified s - d shell Hamiltonian [21] (third column). We also show the band structure in Fig. 2 and their wave function components in Fig. 3.

It can be seen from Fig. 1 that the low-lying energy spectra of ^{21}Ne is well described using the truncated quasi-SU(3) space, which includes only the 17 coupled irreps with the largest C_2 values, out of the 137 coupled irreps (some of them with ρ multiplicity larger than 1) which form the full SU(3) basis.

Despite the very schematic form of Hamiltonian (3) and the missing

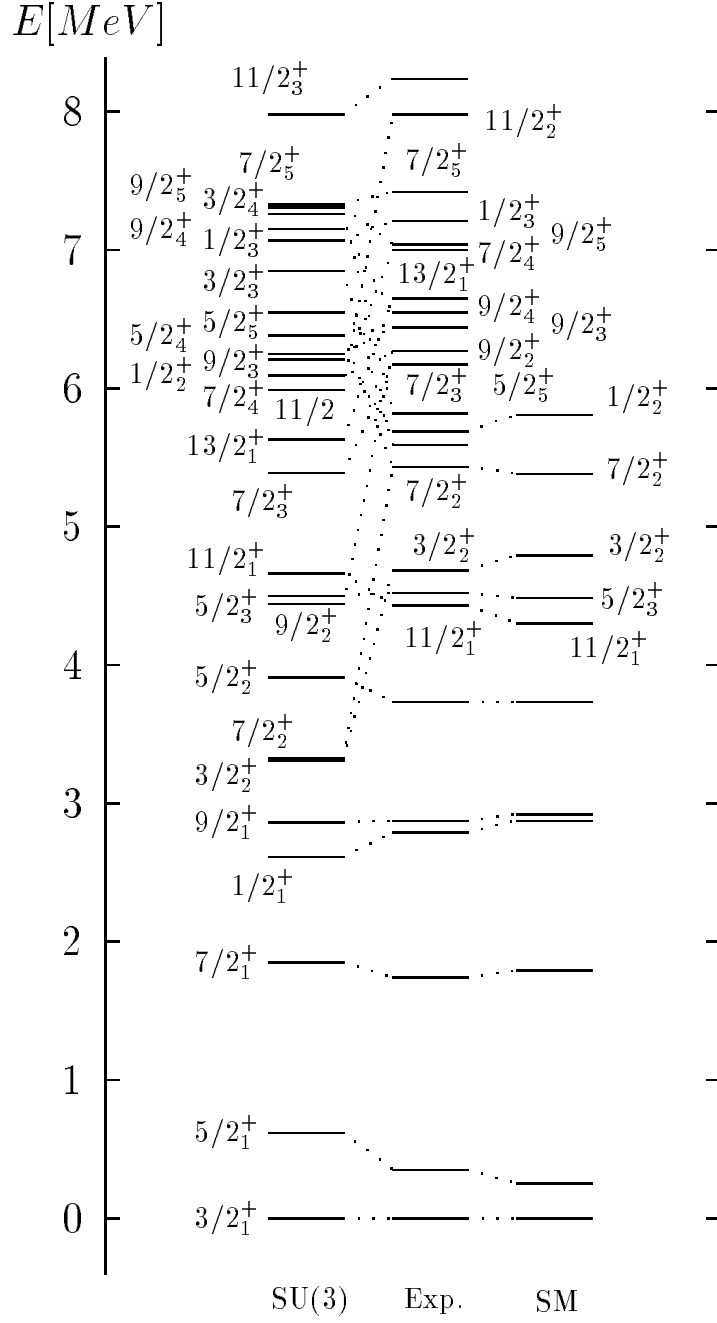


Figure 1: Energy spectrum for ^{21}Ne . The first column displays the present results, the second shows experimental data, and the third column display full shell-model results [21] with a unified sd Hamiltonian [3].

proton-neutron terms mentioned above, the rotor terms allow a fine tuning of the spectra. The moment of inertia is slightly increased by selecting $b = -0.02$. It corrects the quadrupole moment of inertia I , where $1/(2I) = (3/2)\chi \approx 0.16$. Some excited states are moved to higher energies by using $a = -0.200$. Using $A_{sym} = 0.010$ for the symmetry term enhances the contributions of the irreps with λ and μ even relative to the others, because they belong to different symmetry types of the intrinsic Vierergruppe D_2 [22].

It is worth mentioning that, as it was the case in even-even nuclei [12], the main features of the spectra can be obtained by setting all the rotor parameters to zero. On the other hand, if they are values that are too large (in absolute value), the whole band structure is destroyed, and with it the agreement with the observed $B(E2)$ values (see below).

The present model predicts the energies of the ground state band, and the states $1/2_1$, $5/2_2$, $5/2_3$, $11/2_3$, $9/2_{3,6}$, $7/2_5$, and $1/2_2$ pretty close to their experimental counterparts. The ground state band staggering effect forces the states to be clustered by pairs: $(3/2, 5/2)$, $(7/2, 9/2)$, $(11/2, 13/2)$ (see also Fig. 2). It is slightly exaggerated in the last case. The levels $3/2_2$, $7/2_2$, $9/2_2$, $7/2_4$, and $11/2_2$ are predicted at energies around 2 MeV lower than observed. This is a clear limitation of the model, which can be related to the limited and schematic nature of Hamiltonian. Further investigations including proton-neutron pairing would clarify this point. In general, the results reported here represent a clear improvement from previous $SU(3)$ based descriptions [23].

Effective charges $e_{\pi \text{ eff}} = 1.56e$, $e_{\nu \text{ eff}} = 0.56$ were used in the evaluation of $B(E2)$ transition strengths for the three nuclei. $B(E2)$ values calculated with the present model, those obtained by the shell model [21] and experimental ones for ^{21}Ne are shown in Table 4. The agreement with both the experimental and shell model values is in general very good. All but the last transition connect states belonging to the ground state band. The factor 5 deviation found in the $5/2_1^+ \rightarrow 7/2_4^+$ transition seem to reflect effects of the truncation of the Hilbert space.

The ^{21}Ne band structure of this nuclei is presented in Fig. 2. Results for the the ground state and $K = 1/2$ bands are very similar to those found in previous studies [21]. The staggering in the ground state band noted above is clearly seen.

The $SU(3)$ wave function components of each band are shown in Fig. 3. The percentage different $SU(3)$ irreps contribute to each state is plotted as

$B(E2) \uparrow$	Expt.	SU(3)	SM [21]
$3/2_1^+ \rightarrow 5/2_1^+$	1.239 ± 0.155	1.215	1.126
$5/2_1^+ \rightarrow 7/2_1^+$	0.505 ± 0.183	0.710	0.738
$7/2_1^+ \rightarrow 9/2_1^+$	0.387 ± 0.215	0.348	0.391
$9/2_1^+ \rightarrow 11/2_1^+$	0.248 ± 0.165	0.239	0.247
$11/2_1^+ \rightarrow 13/2_1^+$		0.187	0.136
$13/2_1^+ \rightarrow 15/2_1^+$		0.129	0.078
$15/2_1^+ \rightarrow 17/2_1^+$		0.077	0.077
$17/2_1^+ \rightarrow 19/2_1^+$		0.040	0.034
$3/2_1^+ \rightarrow 7/2_1^+$	0.675 ± 0.151	0.688	0.633
$5/2_1^+ \rightarrow 9/2_1^+$	0.906 ± 0.097	0.771	0.728
$7/2_1^+ \rightarrow 11/2_1^+$		0.618	0.707
$9/2_1^+ \rightarrow 13/2_1^+$		0.540	0.564
$11/2_1^+ \rightarrow 15/2_1^+$		0.413	0.422
$13/2_1^+ \rightarrow 17/2_1^+$		0.264	0.318
$15/2_1^+ \rightarrow 19/2_1^+$		0.182	0.215
$5/2_1^+ \rightarrow 7/2_4^+$	0.011	0.002	

Table 4: B(E2) transition strengths for ^{21}Ne in $[e^2b^2 \times 10^{-2}]$.

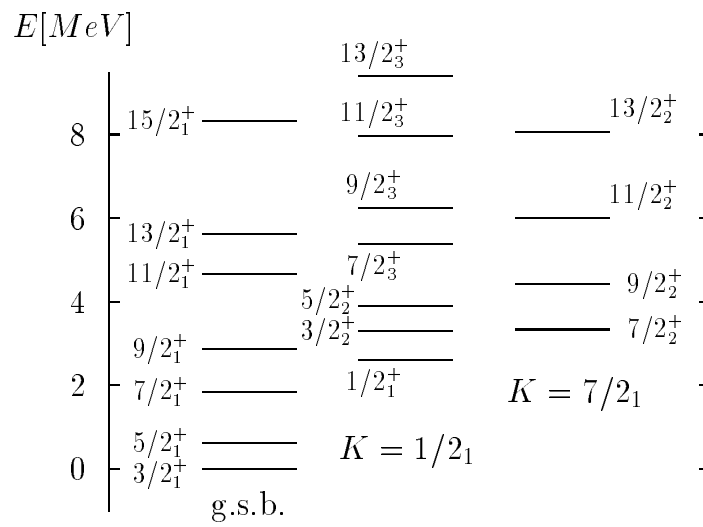


Figure 2: Band structure in ^{21}Ne .

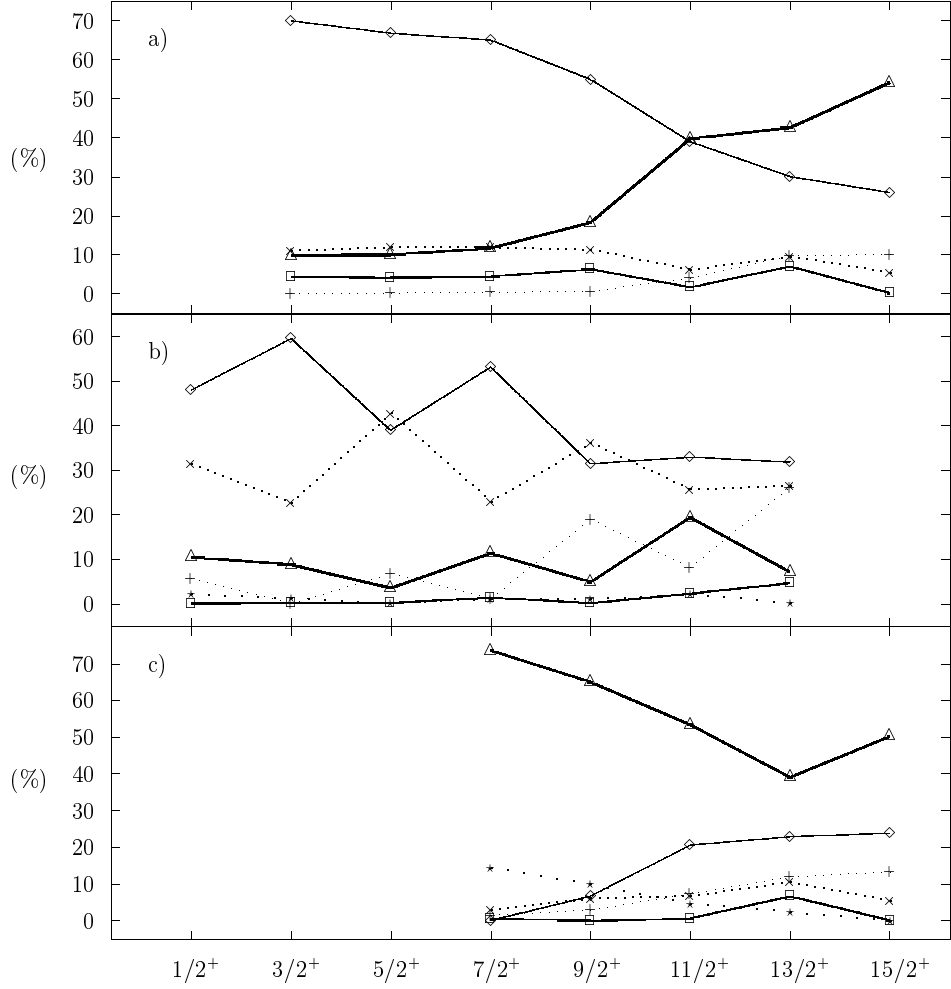


Figure 3: Wave function components of states belonging to a) the ground state band, b) the $K = 1/2$ band and c) the $K = 7/2$ band in ^{21}Ne . The percentage each irrep contributes is shown as function of the angular momentum. The convention used is \diamond for $(8,1)1/2[(4,0)0 \otimes (4,1)1/2]$, $+$ for $(4,3)3/2[(2,1)1 \otimes (2,2)1/2]$, \square for $(7,0)3/2[(4,0)0 \otimes (3,0)3/2]$, \times for $(6,2)1/2[(4,0)0 \otimes (2,2)1/2]$, \triangle for $(6,2)3/2[(2,1)1 \otimes (4,1)1/2]$ and \star for $(4,3)1/2[(2,1)1 \otimes (2,2)1/2]$.

a function of the angular momentum of the members of the band. Different irreps are represented by different lines and symbols (listed in the figure caption). All irreps which contributes more than 2% are plotted. The bands are recognized by their large B(E2) transition strengths. The slow (adiabatic) change in their SU(3) content helps to confirm the band assignment.

Insert a) of Fig. 3 shows the dominance of the irrep (8,1) with spin 1/2 in the ground state band up to $J=9/2$, in agreement with previous studies [23, 24]. At $J = 11/2$ there is a clear change in the wave function, which for $J=13/2, 15/2$ is dominated by the (6,2) irrep with spin 3/2. Irreps with spin $S=3/2$ were not included in [23]. In the present contribution we are showing for the first time its relevance in the low energy spectra. This is the main new feature in the present quasi SU(3) truncation scheme. In [24] it was found that even in presence of strong SU(3) breaking interactions, like the one proposed by Preedom and Wildenthal, there is a clear dominance of the (8,1)1/2 irrep for the ground state, in complete agreement with the present results. In the other two bands, insert b) for $K = 1/2$ and c) for $K = 7/2$ in Fig. 3, similar features can be found. While the $K = 1/2$ band exhibits strong mixing between the (8,1) 1/2 and (6,2) 1/2 irreps, the $K = 7/2$ band is dominated by the (6,2) 3/2 band, underlining once again the crucial role played by spin 3/2 irreps.

4 ^{23}Na

^{23}Na has 11 protons and 12 neutrons. The valence space contains 3 protons and 4 neutrons in the *sd*-shell, allowing for the five proton SU(3) irreps and ten neutron SU(3) irreps listed in Table 5. From them, only three proton irreps and five neutron irreps contribute to the truncated basis, which include the 20 coupled irreps with spin $S= 1/2, 3/2$ listed in Table 6. The complete space contains 670 coupled irreps plus their external multiplicities. Notice that most irreps can have both spins, due to the $1 \otimes 1/2$ coupling. There are also two (7,2) 1/2 irreps, one coming from the $(4,1)1/2 \otimes (3,1)0$ coupling, and the other from the $(4,1)1/2 \otimes (3,1)1$ coupling.

The right hand side of Fig. 4 shows the results obtained for the low energy spectra of ^{23}Na , calculated using the Hamiltonian parameters listed in the second row of Table 2, and the Hilbert space described above. This is compared with the experimental data [20], presented in the second column,

$(\lambda_\pi, \mu_\pi)S_\pi$	C_2	$(\lambda_\nu, \mu_\nu)S_\nu$	C_2
(4,1)1/2	36	(4,2)0	46
(2,2)1/2	24	(5,0)1	40
(3,0)3/2	18	(2,3)1	34
(0,3)3/2	18	(0,4)0	28
(1,1)1/2	9	(3,1)0,1	25
		(1,2)1,2	16
		(2,0)0	10
		(0,1)1	4

Table 5: Irreps, spins and C_2 values for protons and neutrons in ^{23}Na .

(λ_π, μ_π)	(λ_ν, μ_ν)	(λ, μ) total			
(4,1)1/2	(4,2)0	(8,3)1/2	(9,1)1/2	(6,4)1/2	(7,2)1/2
(4,1)1/2	(5,0)1	(9,1)1/2,3/2	(7,2)1/2,3/2		
(4,1)1/2	(2,3)1	(6,4)1/2,3/2	(7,2)1/2,3/2		
(2,2)1/2	(4,2)0	(6,4)1/2	(7,2)1/2		
(4,1)1/2	(3,1)0,1	(7,2)1/2,3/2			
(2,2)1/2	(5,0)1	(7,2)1/2,3/2			
(3,0)3/2	(4,2)0	(7,2)3/2			

Table 6: The 20 irreps used in the description of ^{23}Na .

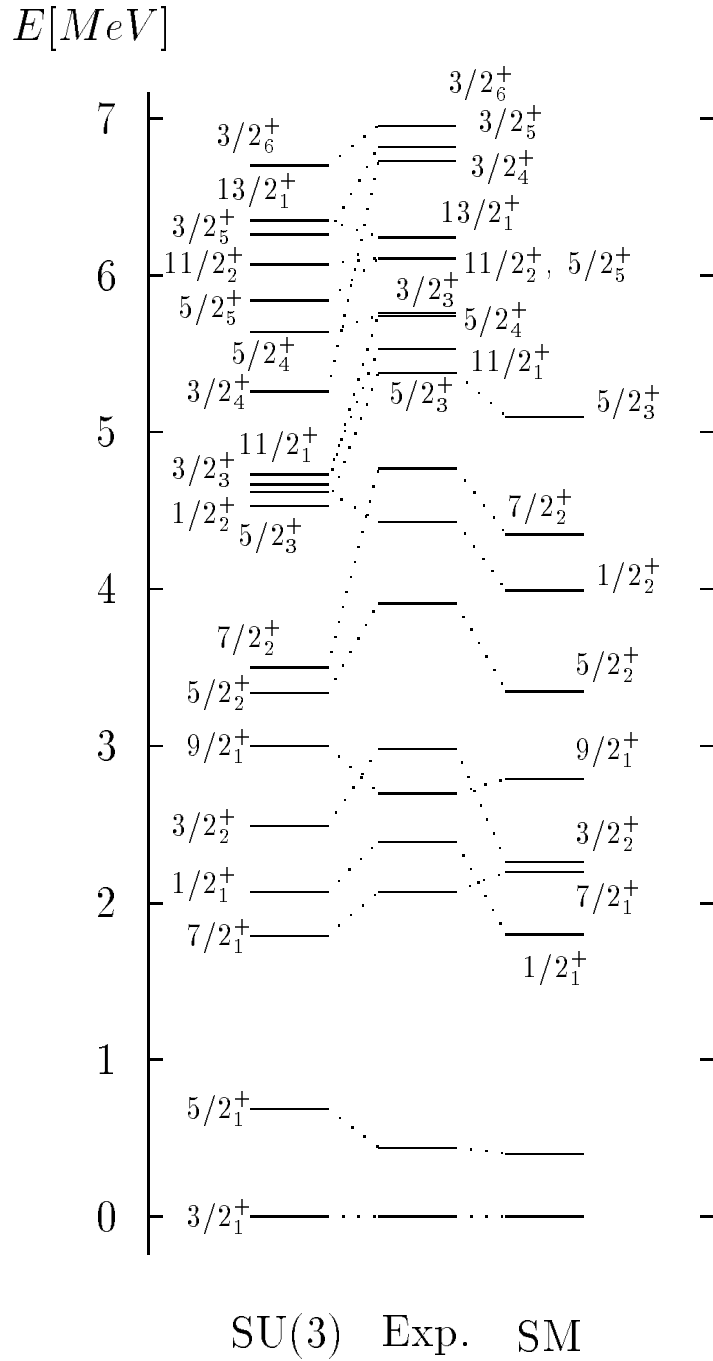


Figure 4: Energy spectrum of ^{23}Na , with the same convention of Fig. 1. The SM data are from Glasgow group [25].

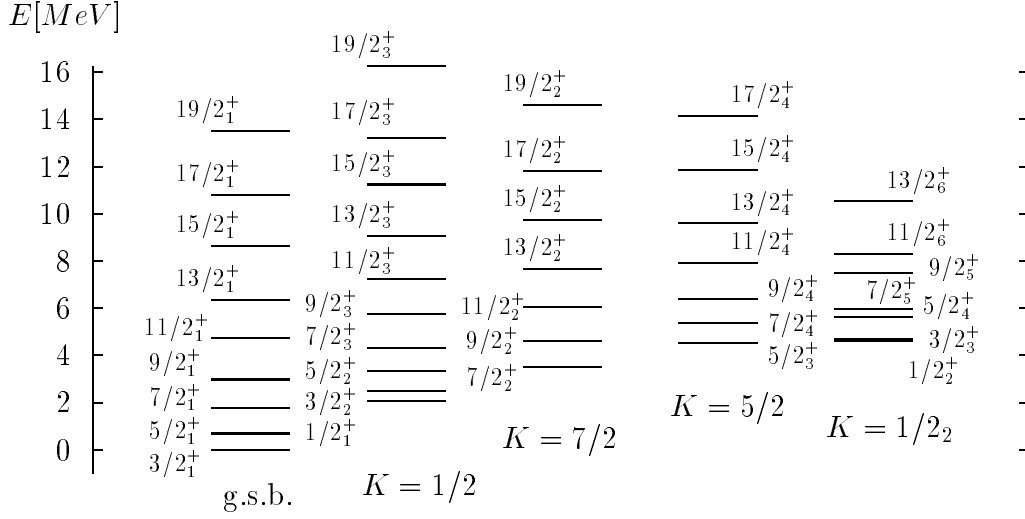


Figure 5: Band structure in ^{23}Na .

and with full shell model calculations performed by the Glasgow group [25] (third column). The ground state, as well as some excited states are well described using the quasi SU(3) truncation scheme. On the other hand, as can be seen in Fig. 4, the model fails to reproduce the energy of the states $7/2_2$, $5/2_3$, $3/2_3$, $3/2_4$, and others, thereby exhibiting the limits of the model. The energy of these states is in general underestimated, probably due to the limited Hamiltonian used.

The band structure, reconstructed from the largest $B(E2)$ calculated values, is shown in Fig. 5. Comparing Figs. 4 and 5 it is noticeable that the ground state band is well described, while the excited $K=1/2$ and $K=7/2$ bands are displaced to lower energies than in the observed spectrum. Adjusting the Hamiltonian parameters did not prove to be useful for correcting this feature, pointing again to the need of including another terms in the Hamiltonian.

The negative parameter $b = -0.005$ provides a small correction to the moment of inertia, which is similar to what was found for ^{21}Ne . The other two rotor parameters were found to be useless in this nuclei. Both tend to

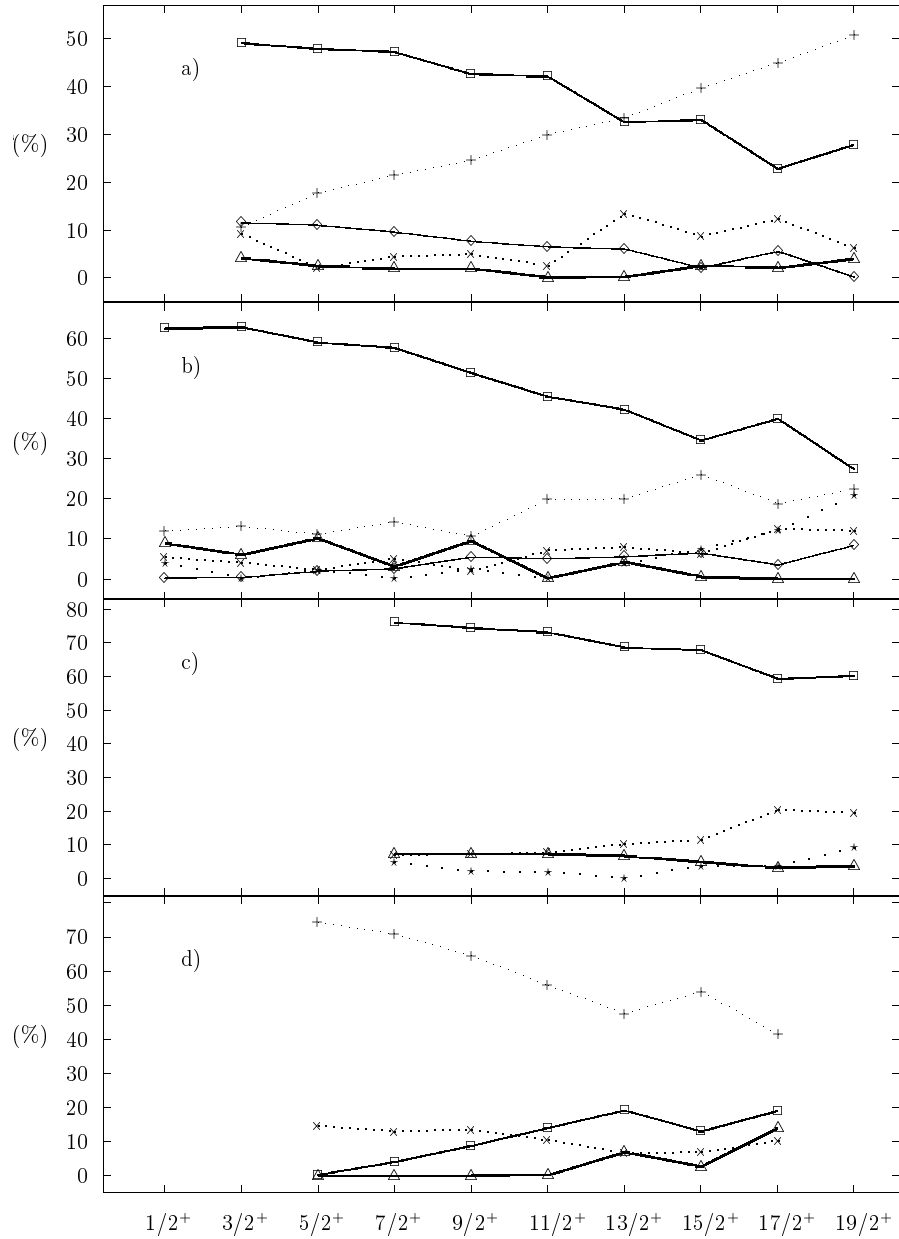


Figure 6: Wave function components of states belonging to a) the ground state band, b) the $K = 1/2$ band, c) the $K = 7/2$ band and d) the $K = 5/2$ band in ^{23}Na . The percentage associated with each irrep is shown as function of the angular momentum. The convention used is \square for $(8,3)1/2[(4,1)1/2 \otimes (4,2)0]$, $+$ for $(9,1)3/2[(4,1)1/2 \otimes (5,0)1]$, \diamond for $(9,1)1/2[(4,1)1/2 \otimes (4,2)0]$, \times for $(7,2)3/2[(4,1)1/2 \otimes (3,1)1]$, \triangle for $(6,4)1/2[(2,2)1/2 \otimes (4,2)0]$ and \star for $(6,4)3/2[(4,1)1/2 \otimes (2,3)1]$.

$B(E2) \uparrow$	Expt.	SU(3)
$3/2_1^+ \rightarrow 5/2_1^+$	1.573 ± 0.233	1.677
$5/2_1^+ \rightarrow 7/2_1^+$	0.777 ± 0.207	1.123
$5/2_1^+ \rightarrow 9/2_1^+$	1.359 ± 0.194	1.031
$3/2_1^+ \rightarrow 7/2_1^+$	0.987 ± 0.085	1.015
$1/2_1^+ \rightarrow 5/2_1^+$	0.124 ± 0.023	0.002
$1/2_1^+ \rightarrow 5/2_2^+$	2.681 ± 0.583	2.103
$7/2_1^+ \rightarrow 9/2_1^+$		0.447
$7/2_1^+ \rightarrow 11/2_1^+$		1.216
$9/2_1^+ \rightarrow 11/2_1^+$		0.512
$9/2_1^+ \rightarrow 13/2_1^+$		0.888
$11/2_1^+ \rightarrow 13/2_1^+$		0.157
$11/2_1^+ \rightarrow 15/2_1^+$		1.055
$13/2_1^+ \rightarrow 15/2_1^+$		0.322
$13/2_1^+ \rightarrow 17/2_1^+$		0.671
$15/2_1^+ \rightarrow 19/2_1^+$		0.800

Table 7: B(E2) transitions for ^{23}Na in [$e^2b^2 \times 10^{-2}$].

wash out the staggering in the ground state band, and also destroy the band structure. For these reasons they were fixed at zero.

It is remarkable that many states are well described, and that in most cases the small deviations with respect to the experimental values show the same trend as the shell model results. Some small energy displacements from the observed data in the ground state band are similar to those found in previous SU(3) studies [26].

A study was also performed using the same Hamiltonian but increasing the basis for 20 to 302 irreps, around 40% of the full space. The energy spectrum showed almost no changes. This is a very strong argument in favor of the quasi SU(3) truncation scheme. The most sizable change happened for the $5/2_1$ state, whose energy was reduced by 200 keV, and thereby approaching the experimental value.

Fig. 6 shows the wave function decomposition of the states belonging to a) the ground state band, b) the $K = 1/2$ band, c) the $K = 7/2$ band and d) the $K = 5/2$ band in ^{23}Na . For each band the percentage associated

with different $SU(3)$ irreps is shown as function of the angular momentum. The ground state band is dominated by the irrep $(8,3) 1/2$ up to $J = 13/2$. For larger angular momentum the irrep $(9,1) 3/2$ has the largest component. The $K = 1/2$ band has a similar structure, but for large angular momentum there is competition between the $(9,1) 3/2$ and $(6,4) 3/2$ irreps to replace the $(8,3) 1/2$, resulting in a strong mixing. The $K = 7/2$ band is dominated by the $(8,3) 1/2$ irrep, while the $K = 5/2$ band is by large made of the $(9,1) 3/2$ irrep.

It must be stressed again that the inclusion of the $(9,1) 3/2$ and other spin $3/2$ irreps is one of the most relevant features of the quasi $SU(3)$ truncation scheme, which accounts for most of its present success, as compared with previous $SU(3)$ studies [26].

$B(E2)$ transition strengths are presented in Table 7. They are compared with the experimental values, available for some transitions between states belonging to the ground state band and to the excited $K = 1/2$ band. The agreement is in general very good. The calculated $B(E2; 1/2_1 \rightarrow 5/2_1)$ value is two orders of magnitude smaller than the experimental one, while $B(E2; 1/2_1 \rightarrow 5/2_2)$ is larger and well reproduced.

5 ^{25}Mg

^{25}Mg has 4 protons and 5 neutrons in the sd -valence shell. The ten proton and 12 neutron irreps in which they can be accommodated are listed in Table 8. From the 1821 proton-neutron coupled $SU(3)$ irreps we selected the 16 with the largest C_2 values to build the truncated Hilbert space. They are shown in Table 8, together with their spin. As in the previous cases, some coupled irreps can have both spin $1/2$ and $3/2$. Only the three proton $SU(3)$ irreps and the four neutron $SU(3)$ irreps with the largest C_2 values were included in the truncated basis.

The low energy spectra of ^{25}Mg is depicted in Fig. 7. The first column shows the predicted levels, in the second one the experimental values and in third one those found in full shell model calculations. Its band structure is shown in Fig. 8 and the percentage each irrep contributes to the wave functions of the ground state, $K = 1/2, 1/2_2, 9/2, 13/2$ and $11/2$ bands is presented in Fig. 9. The Hamiltonian parameters used in this calculation are shown in the last row of Table 2.

$(\lambda_\pi, \mu_\pi)S_\pi$	C_2	$(\lambda_\nu, \mu_\nu)S_\nu$	C_2
(4,2)0	46	(5,1)1/2	49
(5,0)1	40	(2,4)1/2	46
(2,3)1	34	(3,2)1/2,3/2	34
(0,4)0	28	(4,0)1/2	28
(3,1)0,1	25	(1,3)1/2,3/2	25
(1,2)1,2	16	(2,1)1/2,3/2	16
(2,0)0	10	(0,2)1/2,5/2	10
(0,1)1	4	(1,0)3/2	4

Table 8: Irreps, spins and C_2 values for protons and neutrons in ^{25}Mg .

(λ_π, μ_π)	(λ_ν, μ_ν)	(λ, μ) total		
(4,2)0	(5,1)1/2	(9,3)1/2	(10,1)1/2	(7,4)1/2
(4,2)0	(2,4)1/2	(6,6)1/2	(7,4)1/2	(4,7)1/2
(5,0)1	(5,1)1/2	(10,1)1/2,3/2		
(4,2)0	(3,2)1/2,3/2	(7,4)1/2,3/2		
(5,0)1	(2,4)1/2	(7,4)1/2,3/2		
(2,3)1	(5,1)1/2	(7,4)1/2,3/2		
(2,3)1	(2,4)1/2	(4,7)1/2,3/2		

Table 9: The 16 irreps used in description of ^{25}Mg .

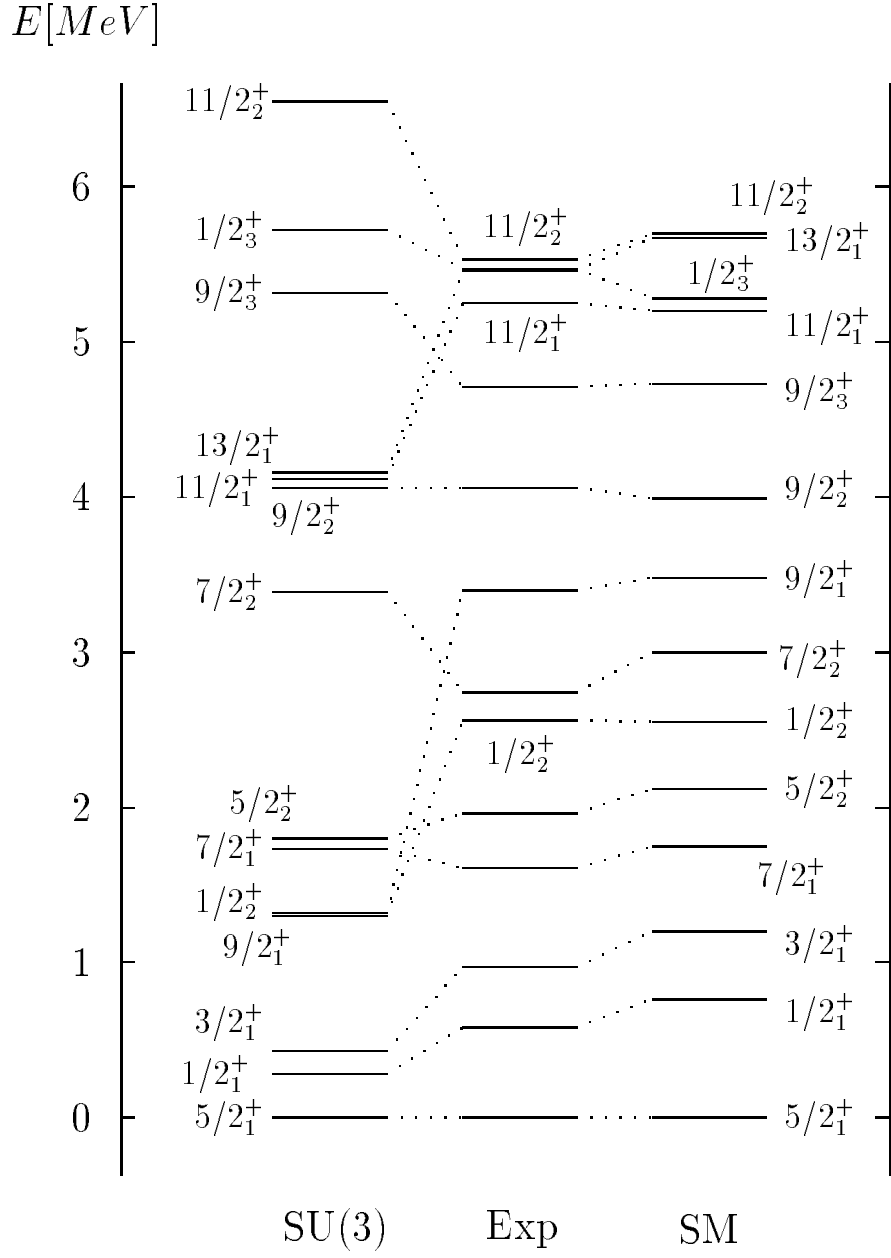


Figure 7: Energy spectra of ^{25}Mg . The first column shows the SU(3) results, the second the experimental levels, and the third the results of full shell model calculations [27].

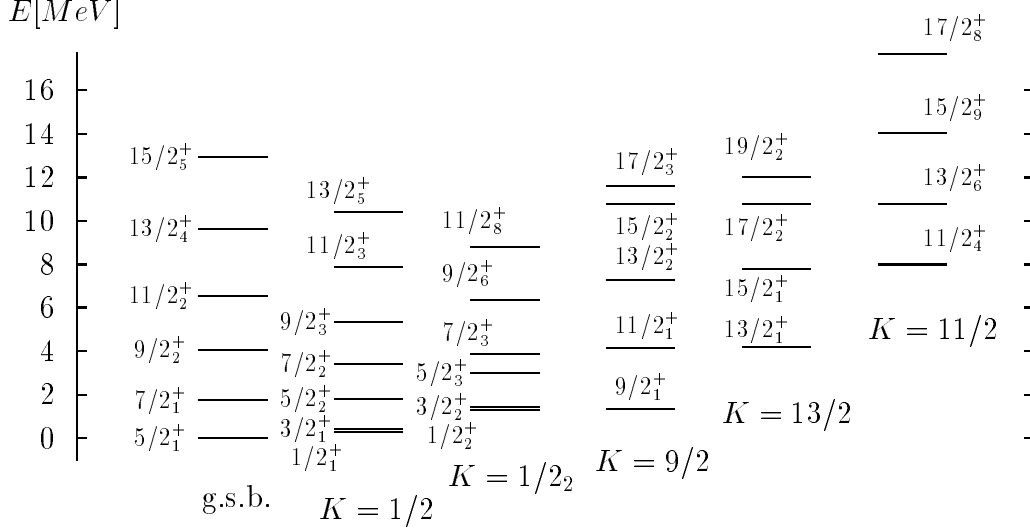


Figure 8: Band structure of ^{25}Mg .

The energy levels shown in Fig. 7 exhibit a complicated pattern. To identify the band structure depicted in Fig. 8, both the $B(E2)$ values and the wave function decomposition were employed. This band structure is fully consistent with the one reported in [28]. While good agreement has been found for a number of states, others like $9/2_1$, $1/2_2$, $11/2_1$, and $13/2_1$ show a deviation from the experimental and shell model values, reflecting a limitation of the present model, probably due both to the Hamiltonian used and the truncation of the Hilbert space.

The description of the ^{25}Mg energy levels and its wave functions in terms of $SU(3)$ irreps reported here is very similar to the one described in the original work of Draayer [29], despite the schematic interaction and the smaller basis used in the present work. It strongly supports the reliability of the quasi $SU(3)$ truncation scheme.

The general structure of the energy spectra in Fig. 7 reproduces some of the observed levels. The limitations of the schematic Hamiltonian used can be gauged by the “band shifts” [28] of three excited bands: those with $K = 1/2_2$, $9/2$ and $13/2$. The effect of other terms in the Hamiltonian, like proton - neutron pairing, in shifting these bands in the right direction will be the

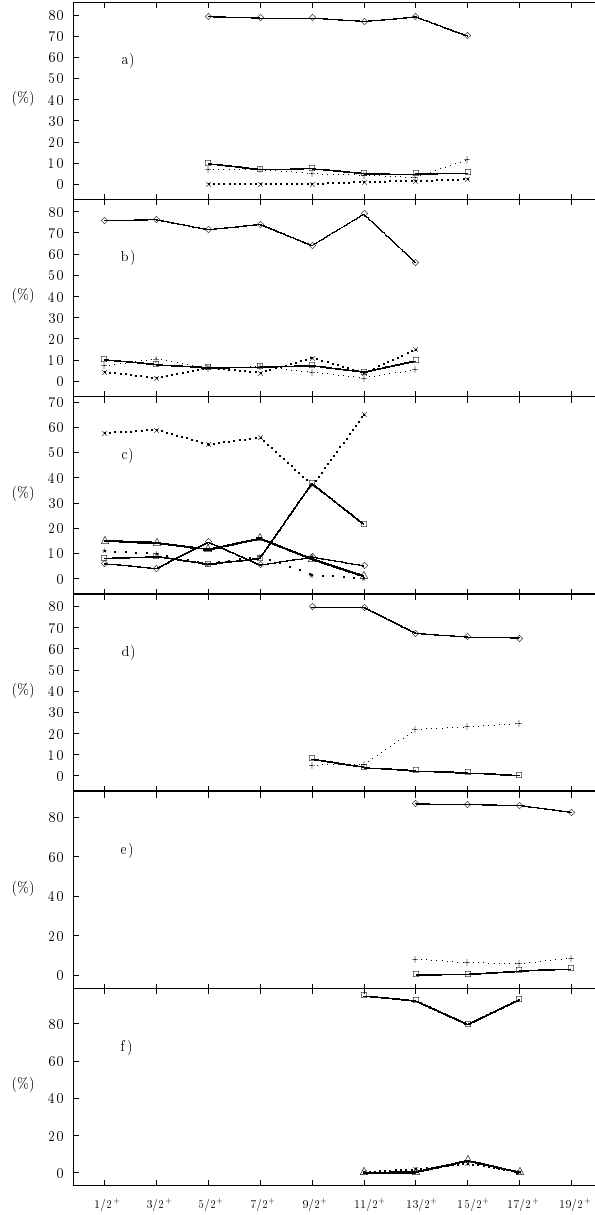


Figure 9: Wave function components of states belonging to a) the ground state band, b) the $K = 1/2$ band, c) the $K = 1/2_2$ band, d) the $K = 9/2$ band, e) the $K = 13/2$ band and f) the $K = 11/2$ band in ^{25}Mg . The percentage each irrep contributes is shown as function of the angular momentum. The convention used is \diamond for $(6,6)1/2[(4,2)0 \otimes (2,4)1/2]$, $+$ for $(4,7)3/2[(2,3)1 \otimes (2,4)1/2]$, \times for $(9,3)1/2[(4,2)0 \otimes (5,1)1/2]$, \triangle for $(10,1)3/2[(5,0)1 \otimes (5,1)1/2]$, \star for $(10,1)1/2[(4,2)0 \otimes (5,1)1]$ and \square for $(7,4)3/2 \{ [(2,3)1 \otimes (5,1)1/2], [(5,0)1 \otimes (2,4)1/2], [(4,2)0 \otimes (3,2)3/2] \}$.

$B(E2) \uparrow$	Exp.	SU(3)	[29]
$1/2_1^+ \rightarrow 5/2_1^+$	0.024 ± 0.001	0.398	0.530
$3/2_1^+ \rightarrow 5/2_1^+$	0.033	0.276	0.180
$1/2_1^+ \rightarrow 3/2_1^+$	0.868 ± 0.434	1.249	1.440
$5/2_1^+ \rightarrow 7/2_1^+$	1.621 ± 0.289	1.968	1.813
$3/2_1^+ \rightarrow 5/2_2^+$	0.202 ± 0.098	0.835	0.510
$1/2_1^+ \rightarrow 5/2_2^+$	2.345 ± 1.042	2.323	2.310
$1/2_2^+ \rightarrow 5/2_1^+$	0.156 ± 0.074	0.020	0.044
$3/2_1^+ \rightarrow 7/2_2^+$	2.084 ± 0.261	1.488	1.540
$5/2_1^+ \rightarrow 7/2_2^+$	0.010	0.001	0.001
$3/2_2^+ \rightarrow 5/2_1^+$	0.074	0.002	0.004
$7/2_1^+ \rightarrow 9/2_1^+$	0.814 ± 0.271	0.081*)	1.362
$5/2_1^+ \rightarrow 9/2_1^+$	0.550 ± 0.043	0.432	0.400
$7/2_1^+ \rightarrow 9/2_2^+$	0.054 ± 0.038	1.420*)	
$5/2_1^+ \rightarrow 9/2_2^+$	0.097 ± 0.006	0.545	
$5/2_2^+ \rightarrow 9/2_3^+$	2.171 ± 0.362	2.066	
$7/2_2^+ \rightarrow 11/2_1^+$	0.847 ± 0.261	0.001	
$7/2_1^+ \rightarrow 11/2_1^+$	0.332 ± 0.078	0.372	
$9/2_1^+ \rightarrow 13/2_1^+$	0.128 ± 0.061	0.279	

Table 10: B(E2) transitions for ^{25}Mg in [$e^2b^2 \times 10^{-2}$]. The second column shows the experimental values, the third column the present theoretical results, and fourth those obtained previously with the SU(3) model [29]. Stars denote transitions with unclear identification in the theory.

subject of future research.

In view of the limitations of Hamiltonian (3), a very specific selection of rotor terms was needed to get a $5/2$ ground state. The parameter set shown in the last line of Table 2 reflects a subtle balance between the J^2 , K^2 and symmetry terms. The negative a value pushes bands with larger K down in energy, while the positive b reduces the moment of inertia, increasing the level separation inside each band, and moving the band heads with larger J to higher energies. Setting $A_{sym} = 0.024$ helps to make the $J = 5/2_1$ state the ground state.

Table 10 lists the B(E2) transitions for ^{25}Mg , calculated with the same effective charges $e_{\pi \text{ eff}} = 1.56e$, $e_{\nu \text{ eff}} = 0.56e$ as used in the previous cases. The second column shows the experimental values, the third column the

present theoretical results, and fourth those obtained previously using the SU(3) model with a renormalized Kuo-Brown interaction [29]. The agreement is in general quite good.

Stars were used to mark the calculated transition strengths $B(E2; 7/2_1 \rightarrow 9/2_1) = 0.081$ ($[e^2b^2 \times 10^{-2}]$) and $B(E2; 7/2_1 \rightarrow 9/2_2) = 1.420$. Due a shift of the $K=9/2$ band, the $9/2_1$ and $9/2_2$ are inverted in our level scheme. A more natural assignment would be $B(E2; 7/2_1 \rightarrow 9/2_1) = 1.420$ and $B(E2; 7/2_1 \rightarrow 9/2_2) = 0.081$, which are close to the experimental results.

Calculated results for the B(E2) transition strengths are not very good. Only a few are well described: $1/2_1^+ \rightarrow 3/2_1^+$, $5/2_1^+ \rightarrow 7/2_1^+$, $1/2_1^+ \rightarrow 5/2_2^+$, $5/2_1^+ \rightarrow 9/2_1^+$, $5/2_2^+ \rightarrow 9/2_3^+$, $7/2_1^+ \rightarrow 11/2_1^+$, and $9/2_1^+ \rightarrow 13/2_1^+$. For the other reported transitions the difference is one or more orders of magnitude, most being underestimated. These wrong predictions show the limitations of the model. It is interesting to see that the present values and those reported in Ref. [29] are in general very close.

As mentioned above, by using the B(E2) transition strengths and the form of the wave function it was possible to identify the six rotational bands shown in Fig. 8, in agreement with [28]. The SU(3) content of these bands is shown in Fig. 9 as a function of the angular momentum of the states belonging to the different bands. Beyond the regular structure found in most of the bands, the most remarkable feature is that of first two bands which have band heads that are dominated by the (6,6) irrep. The “leading” irrep (9,3)1/2 is dominant in the second excited $K=1/2_2$ band. This is a remarkable result: the quadrupole - quadrupole interaction builds the ground state band mostly from the leading irrep. As was pointed out in [29], it also implies a coexistence of prolate and triaxial shapes, associated with the (9,3) and (6,6) irreps, respectively. It also shows that, while developing clear rotational bands, the ^{25}Mg ground state is mostly triaxial. The yrast band, however, includes many different band heads, which are either triaxial or prolate.

At variance from what was found in the lighter nuclei discussed above, the spin 3/2 irreps play only a marginal role in ^{25}Mg , except for the states with the largest angular momentum in the $K = 9/2$ band, insert d), and the $K= 11/2$ band, insert f), which is dominated by the (7,4) 3/2 irrep.

6 Discussion and Outlook

The quasi SU(3) truncation scheme was used in conjunction with Hamiltonian (3) to describe the energy spectra and B(E2) transition strengths in ^{21}Ne , ^{23}Na and ^{25}Mg . Comparison were made with experimental data, with shell model calculations and with previous SU(3) studies. The agreement was in general good, exhibiting the success of the model.

The truncation recipe is quite simple. First select three or four proton and neutron SU(3) irreps with largest C_2 values, which in general will have spin 0 or 1 for an even number of nucleons and spin 1/2 and 3/2 for odd an number of nucleons. Build from these the coupled proton-neutron SU(3) irreps, and select again only a small number with the largest total C_2 values. Usually 20 irreps are enough. Use this basis to diagonalize the Hamiltonian. While the effect of the truncation in ^{21}Ne was small, for ^{25}Mg it implied a two order of magnitude reduction in the basis size. The composition of the calculated wave functions was found to be very similar to the ones reported in previous SU(3) studies with far larger basis where the Kuo interaction was used [29].

The Hilbert space built in this way is rich enough to include many excited rotational bands which have a clear counterpart both in the experimental data and in full shell model calculations. The fact that most of these bands have one fairly dominant SU(3) irrep underscores the strength of the model. This feature leads to a simple picture in terms of the SU(3) decomposition of the wave functions, and exhibits the crossing and mixings which occur within a band as a function of the angular momentum of the different band members. B(E2) transition strengths were also found to be in close correspondence with the experimental data, and this allowed for a clear identification of band members. The SU(3) content of the ground state band also showed that, while ^{21}Ne and ^{23}Na are definitively prolate, ^{25}Mg is mostly triaxial.

There were model limitations uncovered in the present study. The most striking are the band shifts, i.e. the fact that some excited bands are predicted at energies 1 to 2 MeV lower than they appear in the experiment. Given that the band structure and the B(E2) values were in general well depicted, the band shifts seem to reflect on a limitation of the Hamiltonian and not of the Hilbert space, since the same feature was found in full shell model calculations.

It should be clear that Hamiltonian (3) is not missing important two-body

terms. In addition to realistic single particle energies, it includes quadrupole-quadrupole and like particle pairing terms with fixed interaction strengths taken from systematics. It has also three rotor like terms which allow for a fine tuning of the spectra. In the case of ^{25}Mg , these terms played an important role in the reproducing of the energy spectra, especially in pushing the $J = 5/2$ band down to become the ground state band of the system.

In these nuclei with N very close to Z , proton-neutron pairing, both in the $T=0$ and $T=1$ channels, plays a very important role [30]. Its inclusion in Hamiltonian (3) would make it isoscalar. It could be relevant not only for improving the predicted energy spectra, but also in the description of M1 excitations, which are known to be very challenging for any theoretical model [31]. It would also allow the model to be tested in the fp-shell where $B(M1)$ transition strengths have been recently measured [32]. Future research on these subjects is desirable.

7 Acknowledgements

The authors thank C. Johnson and S. Pittel for emphasizing the relevance of proton-neutron pairing in the sd -shell. The authors thank the Institute of Nuclear Theory of the University of Washington for its hospitality and the Department of Energy for partial support during the completion of this work, which was also supported in part by Conacyt (México) and the National Science Foundation under Grant PHY-9970769 and Cooperative Agreement EPS-9720652 that includes matching from the Louisiana Board of Regents Support Fund.

References

- [1] E. Caurier, A. P. Zuker, A. Poves, and G. Martínez-Pinedo, Phys. Rev. **C 50** (1994) 225; A.P. Zuker, J. Retamosa, A. Poves, and E. Caurier, Phys. Rev. **C 52** (1995) R1741; G. Martínez-Pinedo, A. Poves, L. M. Robledo, E. Caurier, F. Nowacki, J. Retamosa, and A. P. Zuker, Phys. Rev. **C 54** (1996) R2150, and G. Martínez-Pinedo, A.P. Zuker, A. Poves, and E. Caurier, Phys. Rev. **C 55** (1997) 187.

- [2] M. G. Mayer, Phys. Rev. **75** (1949) 1969; O. Haxel, J. H. D. Janssen, H. E. Suess, Phys. Rev. **75** (1949) 1766.
- [3] B. H. Wildenthal, Prog. Part. Nucl. Phys. **11** (1984) 5; B. A. Brown, W. A. Richter, K. E. Julies, and B. H. Wildenthal, Ann. Phys. **182** (1988) 191; B. J. Cole, A. Watt, and R. R. Whitehead, J. Phys. A: Math., Nucl. Gen., **7** (1974) 1399.
- [4] I. Schneider, A.F. Lisetskiy, C. Friessner, R.V. Jolos, N. Pietralla, A. Schmidt, D. Weisshaar, and P. von Brentano, Phys. Rev. **C 61** (2000) 044312.
- [5] F. Iachello and A. Arima, *The Interacting Boson Model*, (Cambridge University Press, Cambridge 1987).
- [6] J. P. Elliott, Proc. Roy. Soc. London Ser. A **245** (1958) 128; **245** (1958) 562.
- [7] K. T. Hecht and A. Adler, Nucl. Phys. **A 137** (1969) 129; A. Arima, M. Harvey, and K. Shimizu, Phys. Lett. **B 30** (1969) 517; R. D. Ratna Raju, J. P. Draayer, and K. T. Hecht, Nucl. Phys. **A 202** (1973) 433.
- [8] P. Van Isacker, O. Juillet, and F. Nowacki, Phys. Rev. Lett. **82** (1999) 2060.
- [9] T. Beuschel, J. G. Hirsch, and J. P. Draayer, Phys. Rev. **C 61** (2000) 054307.
- [10] C. E. Vargas, J. G. Hirsch, T. Beuschel, and J. P. Draayer, Phys. Rev. **C 61** (2000) 031301(R); C. E. Vargas, J. G. Hirsch, and J. P. Draayer, Nucl. Phys. **A 673** (2000) 219; J. G. Hirsch, C. E. Vargas, and J. P. Draayer, Rev. Mex. Fis **46 S1** (2000) 54.
- [11] C. E. Vargas, J. G. Hirsch, P. O. Hess, and J. P. Draayer, Phys. Rev. **C 58** (1998) 1488.
- [12] C. E. Vargas, J. G. Hirsch, and J. P. Draayer, arXiv.org/nuc1-th/0009050; Nucl. Phys. A in press.
- [13] C. E. Vargas, J. G. Hirsch, and J. P. Draayer, in preparation.

- [14] M. Moshinsky, *Group Theory and the Many body Problem* (Gordon and Breach, New York, 1967).
- [15] O. Castaños, J. P. Draayer, and Y. Leschber, *Ann. Phys.* **180** (1987) 290; D. Troltenier, C. Bahri, and J. P. Draayer, *Nucl. Phys. A* **586**, (1995) 53; **589**, (1995) 75.
- [16] J. P. Draayer in *Algebraic Approaches to Nuclear Structure* ed. by R. F. Casten *et al.*, (Harwood Academic 89. Publishers, 1993).
- [17] D. Troltenier, J. P. Draayer, and J.G. Hirsch, *Nucl. Phys. A* **601** (1995)
- [18] J. G. Hirsch, P. O. Hess, L. Hdz., C. E. Vargas, T. Beuschel, and J. P. Draayer, *Rev. Mex. Fis.* **45** 2 (1999) 86.
- [19] P. Ring and P. Schuck. *The Nuclear Many-Body problem.*, (Springer, Berlin 1979).
- [20] National Nuclear Data Center, <http://bnlnd2.dne.bnl.gov>
- [21] A. Hoffmann, P. Betz, H. Ropke, and B. H. Wildenthal, *Z. Phys. A*, **332** (1989) 289.
- [22] Y. Leschber, *Hadronic Journal Supplement* **3**, 1 (1987).
- [23] H. A. Naqvi and J. P. Draayer, *Nucl. Phys. A* **526** (1992) 297.
- [24] H. Feldmeier and P. Manakos, *Z. Phys. A* **281** (1977) 379.
- [25] B. J. Cole, A. Watt, and R. R. Whitehead, *J. Phys. A: Math., Nucl. Gen.* **7** (1974) 1374.
- [26] H. A. Naqvi, C. Bahri, D. Troltenier, J. P. Draayer, and A. Faessler, *Z. Phys. A* **351** (1995) 259.
- [27] D. M. Headly, *et. al.* *Phys. Rev.C* **38** (1988) 1698.
- [28] B. J. Cole, A. Watt, and R. R. Whitehead, *J. Phys. G: Nucl. Phys.* **1** (1975) 17.
- [29] J. P. Draayer, *Nucl. Phys. A* **216** (1973) 457.

- [30] S. Krewald, K. W. Schmid, and A. Faessler, *Z. Phys.* 269 (1974) 125.
- [31] J. F. A. Van Hienen, P. W. M. Glaudemans, and J. Van Lidth De Jeude, *Nucl. Phys. A* **225** (1974) 119.
- [32] A. F. Lisetskiy, R. V. Jolos, N. Pietralla, and P. von Bretano, *Phys. Rev. C* **60** (1999) 064310.